

## Modeling the effect of deformation on strength of a Fe-23Mn-0.3C-1.5Al TWIP steel

This content has been downloaded from IOPscience. Please scroll down to see the full text.

2014 IOP Conf. Ser.: Mater. Sci. Eng. 63 012059

(<http://iopscience.iop.org/1757-899X/63/1/012059>)

View [the table of contents for this issue](#), or go to the [journal homepage](#) for more

Download details:

IP Address: 82.151.111.206

This content was downloaded on 11/08/2014 at 14:02

Please note that [terms and conditions apply](#).

# Modeling the effect of deformation on strength of a Fe-23Mn-0.3C-1.5Al TWIP steel

**P Kusakin<sup>1</sup>, A Belyakov<sup>1</sup>, R Kaibyshev<sup>1</sup> and D Molodov<sup>2</sup>**

<sup>1</sup>Belgorod State University, Belgorod, Russia

<sup>2</sup>Institute of Physical Metallurgy and Metal Physics, RWTH Aachen University, 52056 Aachen, Germany

E-mail: [kusakin@bsu.edu.ru](mailto:kusakin@bsu.edu.ru)

**Abstract.** Modeling the effect of deformation on mechanical properties of a Fe-23Mn-0.3C-1.5Al (in wt. %) TWIP steel subjected to extensive cold rolling was performed. The approach including Hall-Petch relation and dislocation strengthening was used for the determination of the strength increment with deformation. Distance between twin boundaries was considered to be the mean free path for dislocation glide in the Hall-Petch relationship. The rate of dislocation accumulation in the TWIP-steel was calculated via the X-ray diffraction (XRD) measurements and compared with direct transmission electron microscopy (TEM) measurements by counting individual dislocations crossing the thin foil surface after small reductions. It was shown that a decrease of the dislocation mean free path by formation of twins with nanoscale thickness is of less importance for the strengthening than an increase of the dislocation density, which was shown to be the major strengthening mechanism. This suggested that twin boundaries were more readily transparent and, therefore, provided less strengthening as compared to ordinary grain boundaries. The developed model has shown a good agreement with the experimental data.

## 1. Introduction

During last years high-Mn steels with twinning induced plasticity (TWIP) effect have been attracted great attention as a new group of materials for structural applications in the automotive industry due to their excellent combination of strength and elongation [1–3]. TWIP steels usually have Mn content of 18–30 wt. % and additional alloying elements such as C, Al and Si. Numerous studies [4–8] have been carried out to understand the work hardening behavior of TWIP steels. It is believed that formation of mechanical twins during deformation leads to an increase in the instantaneous work hardening rate. In other words, twin boundaries act as strong obstacles for dislocation movement. Such behavior results in the ductility improvement by the delay of local necking [9–11]. Several models have been developed for high-Mn TWIP steels in order to describe the evolution of mechanical properties with strain [11–14]. In most of them the strengthening contribution due to the formation of mechanical twins was considered via a reduction of the mean dislocation free path (i.e., the dynamic Hall–Petch effect). Also, it was recently confirmed that twinning is the most important mechanism explaining the high strain-hardening of TWIP steels [15,16]. However, the proposed models describe the evolution of mechanical properties only at rather low strains, e.g. below 0.6 true strain at fracture during tensile test. The aim of the present study was to develop a model capable to describe the change of mechanical properties during cold rolling of high-Mn TWIP steel up to large strains.

## 2. Experimental

A forged plate of a Fe-23Mn-0.3C-1.5Al steel with the chemical composition given in Table 1 was hot rolled from 50 to 10 mm thickness at 1150°C and then annealed at the same temperature for 1 hour. This treatment resulted in the development of a uniform microstructure with an average grain size of 24 μm. The plate samples were cold rolled to final thickness of 8, 6, 4 and 2 mm (rolling reductions were 20, 40, 60 and 80%, respectively). The rolling direction was the same as that in the hot rolling. The dislocation density was determined by analysis of X-Ray diffraction profiles and estimated by counting



individual dislocations crossing the thin foil surface by method described elsewhere [17,18]. An ARL-Xtra diffractometer operated at 45 kV and 35 mA, and the diffraction profiles were collected using Cu K $\alpha$  radiation. Average values of the crystallite size  $d'$  and microstrains  $\langle \varepsilon_{50}^2 \rangle$  were estimated on the basis of the Williamson-Hall plot [19] given by given by the eq. (1):

$$\frac{\beta_s \cos \Theta}{\lambda} = \frac{2 \langle \varepsilon_{50}^2 \rangle \sin \Theta}{\lambda} + \frac{K}{d'} \quad (1)$$

where  $\Theta$  is Bragg angle,  $K$  is the Scherrer constant and  $B_s$  is the full width at the half maximum height (FWHM) of  $K_{\alpha 1}$  line with the correction of instrumental line broadening. In this study, the FWHM values were measured for  $\gamma$ -Fe (111) and (222) reflections. The instrumental line broadening was obtained from the FWHM value ( $B_r$ ) of  $K_{\alpha 1}$  line of an annealed silicon powder and removed from measured FWHM value ( $B_m$ ) of  $K_{\alpha 1}$  line of TWIP-steel on the following eq. [20]:

$$\beta_s^2 = \beta_m^2 - \beta_r^2 \quad (2)$$

The value of the dislocation density  $\rho$  by XRD was calculated from the average values of the crystallite size  $d'$  and microstrain  $\langle \varepsilon_{50}^2 \rangle$  by using the following relationship [21]:

$$\rho = \frac{3\sqrt{2}\pi \langle \varepsilon_{50}^2 \rangle}{d'b} \quad (3)$$

where  $b$  is the Burgers vector ( $b = a/\sqrt{2}$  for FCC structures,  $a$  is the lattice parameter). Two specimens were used for each condition. For structural characterization by a transmission electron microscope (TEM) thin foils of 3 mm diameter were cut out parallel to the RD-ND plane and grinded to 0.1 mm thickness. Then the discs were polished using a double jet TENUPOL-5 electrolytic polisher at voltage of 20 V at room temperature. An electrolyte contained 10% perchloric acid and 90% acetic acid. The foils were examined using the JEOL JEM-2100 TEM operated at an acceleration voltage of 200 kV. The distance between deformation twins was measured by the mean linear intercept method, in which the direction of a measuring line was normal to the twin boundaries. A least 10 TEM micrographs were used for each specimen to obtain relevant statistics. Tensile tests were carried out by using the Instron 5882 testing machine at an ambient temperature on specimens with a gauge length of 16 mm and cross section of 1.5 mm  $\times$  3 mm cut out parallel to the rolling plane. The samples were tested at a strain rate of  $2 \times 10^{-3} \text{ s}^{-1}$  with tensile axis parallel to the rolling axis. Two tensile specimens were used for each condition.

Table 1. Chemical composition of the investigated steel

Element	C	Mn	Al	Si	Cr	S	P	Fe
[wt pct]	0.304	23.1	1.5	0.09	0.08	0.006	0.017	bal.

### 3. Results and discussion

The Fe-23Mn-0.3C-1.5Al TWIP-steel in the annealed state exhibited a relatively low yield stress (YS) of 235 MPa and medium ultimate tensile strength (UTS) of 660 MPa alongside with the excellent total elongation of 0.67 (given as true strain) (Fig. 1). The cold rolling led to increase in both the YS and ultimate tensile strength significantly, whereas ductility decreased with increasing the rolling reduction. The YS, UTS and total elongation depending

on rolling reduction are summarized in table 2 (deformed specimens denoted as CR<sub>x</sub>, where CR means “cold rolled” and *x* indicate a reduction degree in %). The rolling strain is given as true strain.

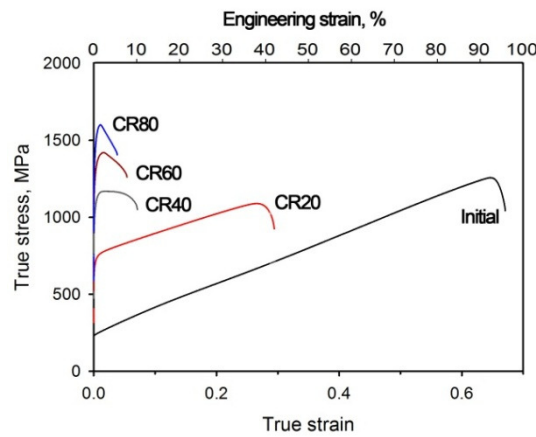


Fig. 1 - The stress-strain curves of the Fe-23Mn-0.3C-1.5Al steel

Table 2 – Chemical composition of the investigated steel

Specimen	Rolling strain	YS, MPa	UTS, MPa	Total elongation
Initial	0	235	660	0.67
CR20	0.22	690	840	0.29
CR40	0.51	1030	1150	0.07
CR60	0.91	1240	1400	0.05
CR80	1.61	1400	1580	0.04

An approach for determination of strength increment with deformation including Hall-Petch relation and dislocation strengthening was used. According to this approach strength increment was calculated as

$$\sigma_{0.2} = \sigma_0 + \frac{K_y}{\sqrt{D}} + \alpha M G b \sqrt{\rho} \quad (4)$$

where  $\sigma_0$  is the friction stress of untwinned matrix,  $K_y$  is the strengthening coefficient,  $D$  is the mean free path for dislocation glide,  $\rho$  is the dislocation density,  $\alpha$  is a constant,  $M$  is the average Taylor factor,  $G$  is the shear modulus, and  $b$  is the Burgers vector. The distance between twin and grain boundaries was considered to be the mean free path for dislocation glide in the Hall-Petch relationship,  $D$ . The rate of dislocation accumulation in the TWIP-steel was calculated using the results of previous X-ray diffraction (XRD) measurements [22] and compared with direct transmission electron microscopy estimation by counting individual dislocations crossing the thin foil surface after small reductions. The experimental values of the distance between twins and the dislocation density estimated by XRD and TEM are given in Table 3. Specimens subjected to high reduction degree were characterized by a high density of deformation twins along with a high dislocation density, such that the dislocation densities were difficult to estimate directly by means of TEM.

Table 3 – Experimental parameters of TWIP-steel microstructure

Specimen	Distance between boundaries, m	$\rho$ [XRD], m <sup>-2</sup>	$\rho$ [TEM], m <sup>-2</sup>	Crystallite size $d'$ , m
Initial	$2.4 \times 10^{-5}$	$10^{14}$	$1.05 \times 10^{14}$	$1.2 \times 10^{-7}$
CR20	$5.7 \times 10^{-7}$	$1.86 \times 10^{15}$	$1.06 \times 10^{15}$	$7.2 \times 10^{-8}$
CR40	$1.83 \times 10^{-7}$	$1.86 \times 10^{15}$	-	$3.5 \times 10^{-8}$
CR60	$1.0 \times 10^{-7}$	$3.44 \times 10^{15}$	-	$4.6 \times 10^{-8}$
CR80	$3.2 \times 10^{-8}$	$4.47 \times 10^{15}$	-	$3.9 \times 10^{-8}$

The measured dislocation densities were approximated by function of exponential growth to maximum as

$$\rho = \rho_0 + \beta(1 - \exp(-ne)) \quad (5)$$

where  $\rho_0$  is the dislocation density in undeformed material,  $e$  is the rolling strain and  $\beta$  and  $n$  are coefficients. The best fit to experimental values was obtained with fitting parameters listed in Table 4. Comparison of experimental and calculated data is shown on Fig. 2.

Assuming that the grain and twin boundaries are main obstacles for dislocation glide,  $D$  in the Hall-Petch relation can be written as [10,23]

$$\frac{1}{D} = \frac{1}{d} + \frac{1}{l} \quad (6)$$

where  $d$  is the mean grain size and  $l$  is the distance between twin boundaries. Taking into account the contribution of specimen's thickness reduction by rolling, Eq. 6 will be written as

$$\frac{1}{D} = \left(\frac{1}{d} + \frac{1}{l}\right) \times \exp(ke) \quad (7)$$

where  $k$  is the fitting coefficient. According to Fullman's analysis [24], the distance between twins is linked to the twin content  $f$  and the thickness of twin lamella,  $t$ , by the relation:

$$l = \frac{1}{2t} \times \frac{f}{1-f} \quad (8)$$

To describe the evolution of distance between twins, simplified equation proposed by Bouaziz [13] was used:

$$f = f_0(1 - \exp(-me)) \quad (9)$$

where  $f_0$  is the maximum fraction of twinned area and  $m$  is the fitting parameter.

As seen in Fig. 3, there is excellent agreement between the mean free path of dislocations calculated according to this model and the current experimental data.

Table 4– values of constants used in Eqs. 5-9

$\rho_0, \text{m}^{-2}$	$\beta, \text{m}^{-2}$	n	$F_0$	t, m	k	m
$10^{14}$	$5.35 \times 10^{15}$	1.1	0.65	$2 \times 10^{-8}$	0.6	0.43

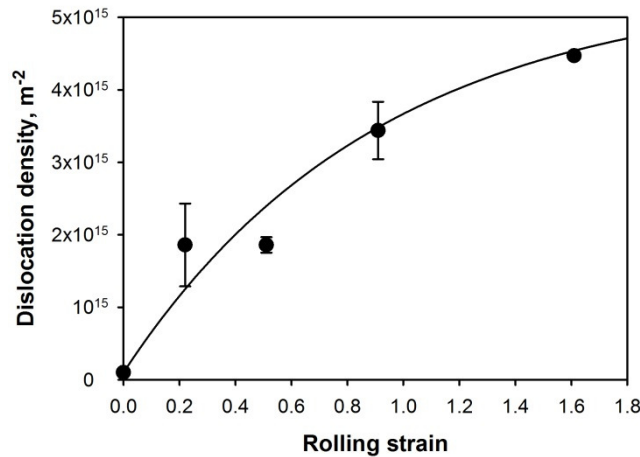


Fig. 2 – Experimental (dot) and calculated (line) values of dislocation densities of the present TWIP-steel.

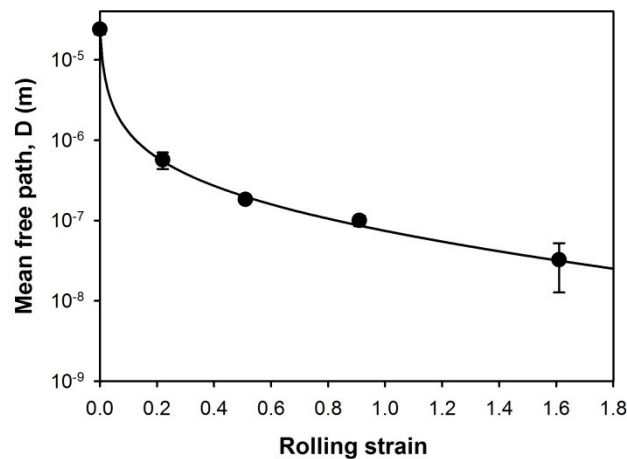


Fig. 3 – Experimental (dot) and calculated (line) values of distance between twins of the investigated TWIP-steel.

After substitution of  $\rho$  and  $D$  from Eq. 5 and Eq. 7 into Eq. 4 and coefficients from Table 4, the flow stress can be written as:

$$\sigma_{0.2} = \sigma_0 + K_y \left( \frac{\exp(16.601 + 0.6e) - \exp(16.5985 + 0.17e)}{0.35 + \exp(-0.43(1 + e))} \right)^{-0.5} + \alpha M G b \sqrt{10^{14} + 5.35 \times 10^{15} (1 - \exp(-1.1e))} \quad (10)$$

The best agreement between the flow stress by Eq. 4 and the experimental data was achieved with constants given in Table 5, though parameters listed in Table 4 were used for the best fit to dislocation densities from experiment. It should be noted that dislocation densities calculated with  $\rho_0$ ,  $\beta$  and  $n$  from Table 5 have only minor difference with values measured with constants from Table 4.

Table 5 – values of constants used in Eq. 4

$\rho_0, \text{m}^{-2}$	$\beta, \text{m}^{-2}$	$n$	$\sigma_0, \text{MPa}$	$K_y, \text{MPa} \times \text{m}^{0.5}$	$\alpha$	$M$	$G, \text{MPa}$	$b, \text{m}$
$5 \times 10^{13}$	$5.75 \times 10^{15}$	1.03	110	0.025	0.33	3	72000	$2.4 \times 10^{-10}$

Hence, Eq. 4 can be written as:

$$\sigma_{0.2} = 110 + \left( \frac{\exp(9.223 + 0.6e) - \exp(9.2207 + 0.17e)}{0.35 + \exp(-0.43(1 + e))} \right)^{-0.5} + 17.1 \times 10^7 \sqrt{58 - \exp(4.05 - 1.03e)} \quad (11)$$

Thereby strength contribution by the Hall-Petch effect is much less than that of the dislocation density. Fig. 4 illustrates contribution of each mechanism to the tensile strength of the Fe-23Mn-0.3C-1.5Al TWIP-steel and Fig. 5 shows a good agreement between the calculated and experimental data. Here  $\sigma_{\text{HP}} = K_y D^{-0.5}$  and  $\sigma_{\text{disl}} = \alpha M G b \rho^{0.5}$ .

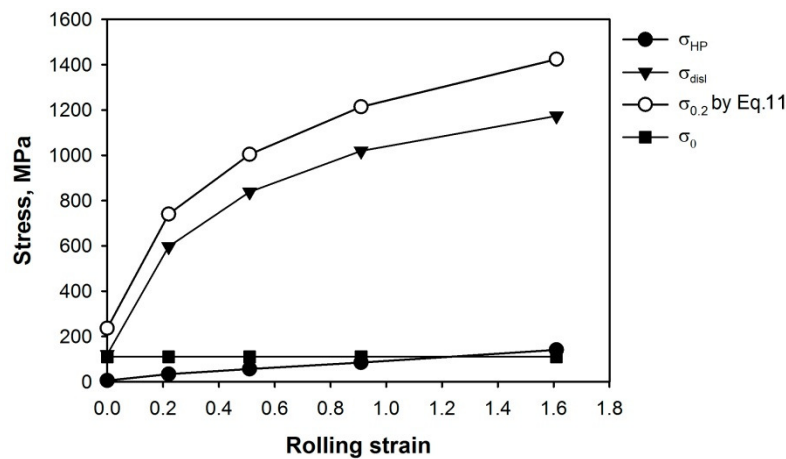


Fig. 4 – Calculated strength contribution of the present TWIP-steel by different mechanisms.

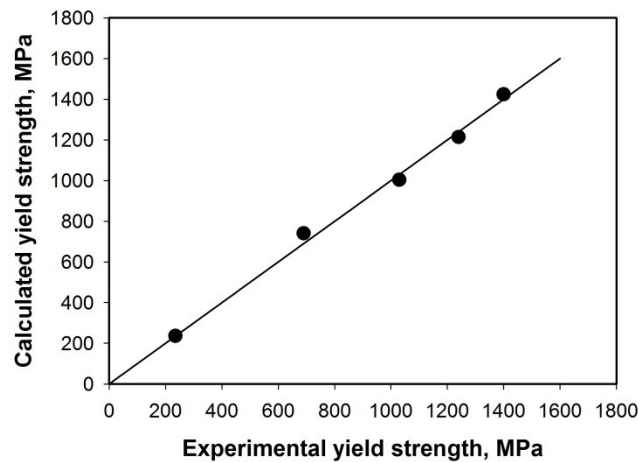


Fig. 5 – The relationship between the experimental and calculated values of yield strength.

Eq. 11 represents a modified type of the equation proposed by Voce [25]:

$$\sigma = B - (B - A)\exp(-n\epsilon) \quad (12)$$

The same type of relationship was found by Nguyen Q. Chinh and T.G. Langdon [26] in pure aluminum and pure copper over a wide range of strains through a combination of conventional tensile and compressive testing and the use of samples processed by equal-channel angular pressing (ECAP) to high strains at different temperatures.

#### 4. Conclusions

1. Modeling the effect of deformation on mechanical properties of a Fe-23Mn-0.3C-1.5Al (in wt. %) TWIP steel subjected to extensive cold rolling was addressed. Cold rolling led to an increase of dislocation density and decrease of dislocation mean free path resulted from mechanical twinning and rolling reduction. Dislocation density evolution can be written as  $\rho = 5 \times 10^{13} + 5.75 \times 10^{15} \times (1 - \exp(-1.03\epsilon))$  and dislocation mean free path dependence on rolling strain can be written as

$$D = \frac{0.35 + \exp(-0.43(1 + \epsilon))}{\exp(16.601 + 0.6\epsilon) - \exp(16.5985 + 0.17\epsilon)}$$

2. The model including Hall-Petch relation and dislocation strengthening was proposed and showed good agreement with experimental data.

3. According to the proposed model a decrease of the dislocation mean free path by mechanical twinning had less influence on strengthening of TWIP-steel in comparison with the dislocation strengthening.

#### 5. Acknowledgements

The financial support received under grant N<sup>o</sup>2014/420 is gratefully acknowledged. One of the authors (DM) expresses his gratitude to the Deutsche Forschungsgemeinschaft (DFG) for financial support within the Collaborative Research Centre (SFB) 761 “Stahl ab-initio. Quantenmechanisch geführtes Design neuer Eisenbasiswerkstoffe”. The authors are grateful



to the personnel of the Joint Research Centre, Belgorod State University, for their assistance with instrumental analysis.

## 6. References

- [1] Bouaziz O et al 2011 *Curr. Op. in Solid State and Mater. Sci.* vol 15 pp 141–168
- [2] De Cooman BC et al 2011 *New Trends and Developments in Automotive System Engineering* ed Marcello Chiaberge (InTech) chapter 6 pp 101–128
- [3] Grassel O et al 2000 *Int. J. Plast.* vol 16 pp 1391–1409
- [4] Asgari S et al 1997 *Metall. Mater. Trans. A* vol 28 pp 1781–1795
- [5] Salemi AA et al 2006 *Metall. Mater. Trans. A* vol 37 pp 259–268
- [6] Hamdi F and Asgari S 2008 *Metall. Mater. Trans. A* vol 39 pp 294–303
- [7] Yang HK, Zhang ZJ and Zhang ZF 2013 *Scripta Mater.* vol 68 pp 992–995
- [8] Bouaziz O 2009 *Scripta Mater.* vol 60 pp 714–716
- [9] Kocks UF and Mecking H 2003 *Prog. Mater. Sci.* vol 48 pp 171–273
- [10] Bouaziz O and Guelton N 2001 *Mater. Sci. Eng. A* vol 319–321 pp 246–249
- [11] Allain S et al 2004 *Mater. Sci. Eng. A* vol 387–389 pp 272–276
- [12] Dini G 2010 *Mater. Sci. Eng. A* vol 527 pp 2759–2763
- [13] Bouaziz O 2008 *Scripta Mater.* vol 58 pp 484–487
- [14] Bouaziz O 2012 *Scripta Mater.* vol 66 pp 982–985
- [15] Kim JK et al 2010 *Mater. Sci. Forum* 2010 vol 654–656 pp 270–273
- [16] Kim JK et al 2009 *Metall. Mater. Trans. A* vol 40 pp 3147–3158
- [17] Kaibyshev R et al 2005 *Mater. Sci. Eng. A* vol 396 pp 341–351
- [18] Hirsch PB et al 1977 *Electron Microscopy of Thin Crystals second ed.* (New York: Krieger)
- [19] Williamson GK, Hall WH 1953 *Acta Metall.* vol 1 pp 22–31
- [20] Warren BE, Biscoe J 1938 *J. Am. Ceram. Soc.* vol 21 pp 49–54
- [21] Smallman RE and Westmacott KH 1957 *Philos. Mag.* vol 2 pp 669–683
- [22] Kusakin P, Belyakov A, Kaibyshev R and Molodov D 2013 *Advanced Materials Research* vol. 922 (2014) pp 394–399
- [23] Estrin Y and Mecking H 1984 *Acta Metall.* vol 32 pp 57–70
- [24] Fullman RL 1953 *Trans. of AIME* vol 197 pp 447–452
- [25] Voce E 1948 *J. Inst. Metals* vol 74 pp 537–562
- [26] Chinh NQ 2004 *Acta Mater.* vol 52 pp 3555–3563